Int J Earth Sci (Geol Rundsch) (2016) 105:2253–2272
DOI 10.1007/s00531-015-1285-9

ORIGINAL PAPER

Lithological and structural characterization of the Longmen Shan fault belt from the 3rd hole of the Wenchuan Earthquake Fault Scientific Drilling project (WFSD-3)

Haibing Li[1,2] · Huan Wang[1,2] · Guang Yang[3] · Zhiqin Xu[1,2] · Tianfu Li[1,2] · Jialiang Si[1,2] · Zhiming Sun[4] · Yao Huang[5] · Marie-Luce Chevalier[1,2] · Wenjing Zhang[1,2] · Jiajia Zhang[1,2,3]

Received: 14 April 2014 / Accepted: 3 December 2015 / Published online: 14 December 2015

Abstract Drilling in an active fault quickly after a large earthquake is an effective way to study earthquake mechanisms. In order to better understand the mechanical, physical, and chemical characteristics of the faults that ruptured during the 2008 Wenchuan earthquake (Mw 7.9), six boreholes were drilled on the two main strands (Yingxiu–Beichuan and Guanxian–Anxian faults) by the Wenchuan earthquake Fault Scientific Drilling project (WFSD). This paper focuses on the cores from the WFSD-3 borehole which drilled across the Guanxian–Anxian fault. A detailed petrological study shows that fault gouge and fault breccia are developed in the WFSD-3 cores in the Late Triassic Xujiahe Formation. The thicknesses of fault gouge range from ~1 mm to ~2.3 m. According to the characteristics of the fault rock combinations and their distribution, at least 22 subsidiary fault zones were recognized in the WFSD-3 cores. The Guanxian–Anxian fault zone is composed of fault rocks from 1192 to 1250.09 m depth, with a real thickness of ~50 m (~60 m thick in the WFSD-3 cores), and an actual damage zone of ~160 m (~980–1192 m depth in the WFSD-3 cores), and shows characteristics of multiple high-strain fault cores. The damage zone is only present in the hanging wall. The actual total thickness of the Guanxian–Anxian fault zone is ~210 m. Based on the analyses of comprehensive logging data, characteristics of the fault gouge, and seismic fault structures, the principal slip zone for the Wenchuan earthquake is identified in the black fault gouge at 1249.95 m depth in the cores, which lies almost at the bottom of the Guanxian–Anxian fault zone, and is also confirmed by surface rupture zone observations. The slip plane of the Wenchuan earthquake is a low-angle thrust fault with a dip angle of ~38° as estimated from the results of the WFSD-3 core analyses. The results from WFSD-1 showed that the Yingxiu–Beichuan segment is a high-angle thrust fault striking NW with a dip angle of ~65°. These two fault segments have different thicknesses and fault structures, which may suggest different faulting mechanisms and evolution history.

Keywords Wenchuan earthquake Fault Scientific Drilling project (WFSD) · Guanxian–Anxian fault zone · Principal slip zone (PSZ) · WFSD-3

Introduction

Drilling in an active fault immediately after a large earthquake is one of the most effective methods to capture direct information for seismic fault, which can yield geological, geophysical, and geochemical data that may help answer fundamental questions about the physical mechanisms of fault slip (Zoback et al. 2007; Xu et al. 2008; Brodsky et al. 2009). In particular, accurate measurements of physical parameters, such as temperature, seismic wave velocity, and permeability variation, may be helpful to obtain information about earthquake fault healing and rupture cycles, seismic frictional heat, permeability, fluid effect, and stress

✉ Haibing Li
lihaibing06@163.com

1 Key Laboratory for Continental Dynamics of the Ministry of Land Resources, Beijing 100037, China

2 Institute of Geology, Chinese Academy of Geological Sciences, Beijing 100037, China

3 Chengdu University of Technology, Chengdu 610059, China

4 Institute of Geomechanics, Chinese Academy of Geological Sciences, Beijing 100081, China

5 No.6 Brigade of Jiangsu Geology and Mineral Resources Bureau, Lianyungang 222300, China

state (Brodsky et al. 2009). Fault rocks retrieved from the drill holes can provide mechanism information, such as earthquake fault slip properties, fracture energy, and friction coefficient (Ma et al. 2006). The Nojima Fault Probe Project pioneered the concept of rapid response drilling following the 1995 Kobe earthquake (Mw 6.9) in Japan (Oshiman et al. 2001), the Taiwan Chelungpu Fault Drilling Project was conducted 5 years after 1999 Chi–Chi earthquake (Mw 7.6) (Ma et al. 2006; Song et al. 2007), the Wenchuan earthquake Fault Scientific Drilling Project (WFSD) was carried out quickly after the 2008 Wenchuan earthquake (Mw 7.9) on November 6, 2008 (just 183 days after the earthquake) (Li et al. 2013), and the Japan Trench Fast Drilling Project (J-FAST) was initiated in 2012 following the March 2011 Tohoku earthquake (Mw 9.0) (Chester et al. 2013). The implementation of these projects has greatly deepened and improved our understanding of earthquake rupture mechanisms.

The May 12, 2008 Wenchuan earthquake (Mw 7.9) occurred along the Longmen Shan fault belt at the transition zone between the eastern margin of the Tibetan Plateau and the Sichuan basin, producing ~270 and ~80 km of coseismic surface ruptures along the Yingxiu–Beichuan and Guanxian–Anxian faults, respectively (Fu et al. 2008, 2011; Li et al. 2008; Liu et al. 2008; Xu et al. 2009). WFSD has drilled six holes (WFSD-1, WFSD-2, WFSD-3, WFSD-3P, WFSD-4, and WFSD-4S) at different sites, with four holes along the Yingxiu–Beichuan fault (WFSD-1, WFSD-2, WFSD-4, and WFSD-4S) and two additional holes along the Guanxian–Anxian fault (WFSD-3 and WFSD-3P). We obtained preliminary results on the lithological and structural characteristics of the Yingxiu–Beichuan fault by retrieving fault zone rocks from WFSD-1, and were able to determine the location of the principal slip zone (PSZ) for the Wenchuan earthquake, as well as its characteristics (Li et al. 2013, 2014). However, we need to obtain the characteristics of both Wenchuan faults in order to fully understand seismogenic fault characteristics and mechanisms of the Wenchuan earthquake.

Here, based on the strata, lithology, logging data, and structure characteristics of the WFSD-3 drilling cores, we analyze and discuss the characteristics of the Guanxian–Anxian fault, which may help to understand the complete mechanism of such a catastrophic earthquake in the Longmen Shan fault belt.

Geological setting

Longmen Shan fault belt and surface rupture zone of the Wenchuan earthquake

The Longmen Shan fault belt is mainly composed of three NE-striking thrust faults: the Wenchuan–Maoxian, Yingxiu–Beichuan, and Guanxian–Anxian faults, from west to east, respectively. The Longmen Shan region can be divided into four sections by the three faults: Paleozoic metamorphic terrain, Neoproterozoic Pengguan complex, Triassic coal-bearing strata, and Jurassic–Cretaceous foreland basin (Li et al. 2006). The Longmen Shan fault zone has a long history, and its currently active faults have developed along preexisting faults since the Late Triassic (Burchfiel et al. 1995; Li et al. 2006; Densmore et al. 2007; Xu et al. 2008). There are no historical records of Ms > 7.0 earthquakes in the Longmen Shan fault belt before the Wenchuan earthquake, which means that the region had experienced a relatively long quiet period and accumulated adequate strain energy to generate a large earthquake.

The Wenchuan earthquake ruptured the Yingxiu–Beichuan and Guanxian–Anxian faults simultaneously, which were characterized by simple thrust faulting coupled with dextral slip and pure thrusting features, respectively (Fu et al. 2008, 2011; Li et al. 2008; Liu et al. 2008; Xu et al. 2009). Also, a 6-km-long, NE-striking surface rupture zone characterized by thrusting from SW to NE with left-lateral strike-slip component can be seen near Xiaoyudong town (Li et al. 2008; Liu et al. 2008; Xu et al. 2009), which connected the two rupture zones mentioned above. Detailed field investigations show that there are two peaks of vertical offset along the Yingxiu–Beichuan surface rupture zone. To the south, the maximum value is 6–6.7 m in Shenxigou and Bajiaomiao villages (Hongkou county) (Fu et al. 2008, 2011; Li et al. 2008; Liu et al. 2008; Xu et al. 2009). To the north, the maximum value is 11–12 m at Shaba village (Beichuan county) (Li et al. 2008, 2009; Liu et al. 2008; Fu et al. 2009). The maximum vertical offset along the Guanxian–Anxian fault is ~4 m in Qingquan village (Jiulong county, Mianzhu) (Li et al. 2008; Liu et al. 2008; Xu et al. 2009; Fu et al. 2011) with pure thrusting characteristics. The WFSD-3 borehole site is located ~1400 m west of the maximum vertical displacement area (Fig. 1) along the Guanxian–Anxian fault. Viewed from the geological and seismic reflection profiles (Fig. 2), the Guanxian–Anxian fault is a low-angle thrust fault (Lu et al. 2012) which caused Paleozoic strata to be overthrust over the Mesozoic strata.

Strata features near the WFSD-3 drilling site

The WFSD-3 borehole is located in the hanging wall of the Guanxian–Anxian fault in the Triassic Xujiahe Formation (Fig. 3). In the hanging wall, the strata, from older to younger, are mainly composed of the gray to dark-gray Triassic sedimentary rocks: Feixianguan Formation (T_1f) (limestone and mudstone), Jialingjiang Formation (T_2j) (dolomite, siltstone, and limestone), Leikoupo Formation (T_2l) (thick layer dolomite and some mudstone),

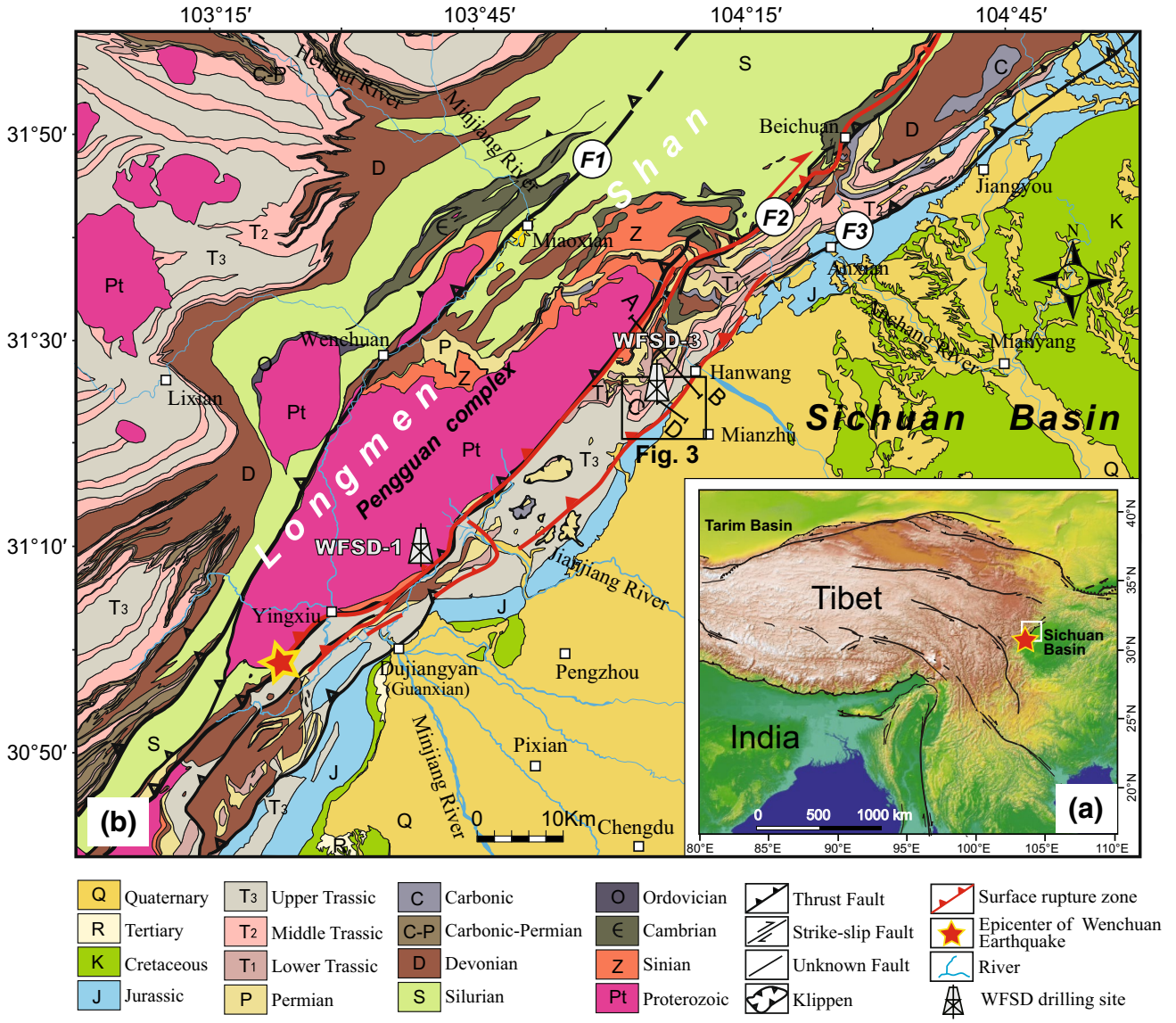

Fig. 1 Tibetan plateau landform (**a**) and geological structures of the Longmen Shan and its adjacent area (**b**) (by Sichuan Bureau of Geology, 1:200000 geologic map of Guangxian) and WFSD drilling sites location. *F1* Wenchuan–Maoxian fault (W-M F.); *F2* Yingxiu–Beichuan fault (Y-B F.); *F3* Guanxian–Anxian fault (G-A F.); Pingwu–Qingchuan fault (P-Q F.) (Li et al. 2013). A–B and C–D profiles are shown in Figs. 2 and 14, respectively

Tianjingshan Formation (T_2t) (bioclastic limestone), Ma'antang Formation (T_3m) (mudstone, limestone, calcareous shale), and Xujiahe Formation (T_3x) (coal-bearing sandstone, siltstone, shale), according to the 1:50,000 geological map of the Mianzhu area (Sichuan Bureau of Geology and Mineral Resources 1996) (Fig. 3). The Xujiahe Formation (T_3x) can be divided into three sections: The lower segment (T_3x^1) is composed of feldspathic quartz sandstone and thin-layer interbedding siltstone, with some marlstone; the middle segment (T_3x^2) consists of lithic quartz sandstone, siltstone with marlstone, and carbonaceous shale; the upper segment (T_3x^3) consists of lithic sandstone and siltstone interbedded, carbonaceous shale, and coal lines. The footwall of the Guanxian–Anxian fault is mainly reddish-brown to grayish-green Jurassic and Quaternary strata. The Jurassic strata are more than 1900 m thick, which formed mainly by a Molasse Formation in the foreland basin edge, and a reddish-brown to grayish-green terrigenous clastic bearing flysch formation, consisting of the Shaximiao Formation (Js), Suining Formation (Jsn), and Lianhuakou Formation (Jl), from lower to upper strata. The Quaternary strata mainly consist of riverbed and flood plain alluvial–pluvial layers and slope alluvium. Viewed in the surface outcrop, there are obvious differences in color and lithology between the hanging wall and footwall.

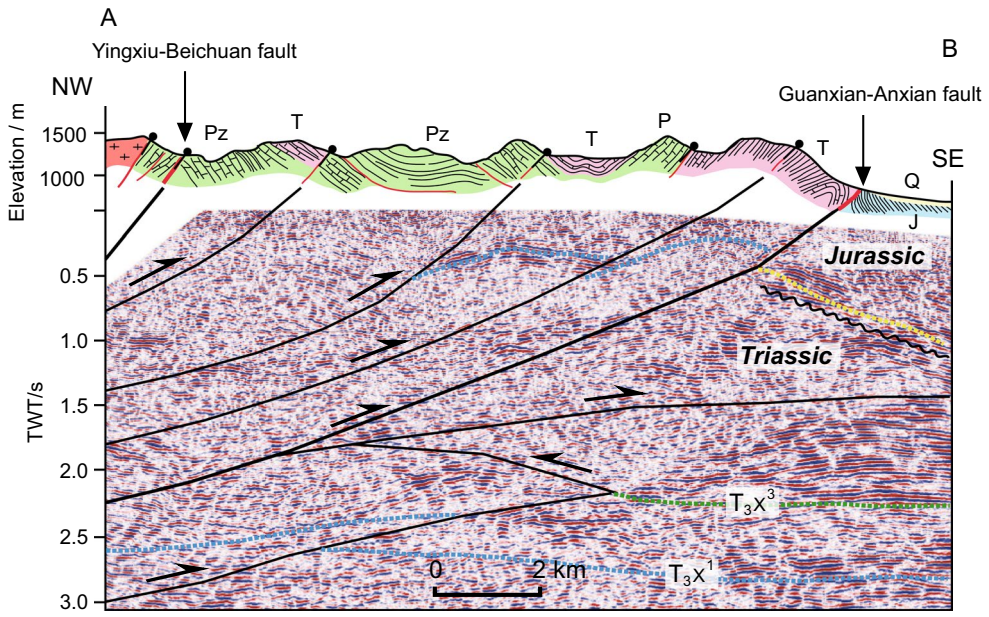

Fig. 2 Geological and geophysical (Lu et al. 2012) profiles (A–B) across the Guanxian–Anxian fault (the location of this profile refers to Fig. 1)

Drilling overview

The WFSD-3 drilling site is located at N31°23′50.24″, E104°06′10.07″ at an altitude of 850, ~1150 m away from the surface rupture zone. Viewed from the seismic reflection profiles across the Guanxian–Anxian fault (Fig. 2), the dip of the Guanxian–Anxian fault is 40°–50° within 2 km from the surface, indicating that WFSD-3 would encounter the Wenchuan earthquake PSZ at 1100–1300 m depth. Therefore, the WFSD-3 was designed to be 1500 m deep.

The WFSD-3 drilling started on December 8, 2009 and ended on February 21, 2012 with a final depth of 1502.30 m, apex angle of 7.6° and azimuthal angle of 203°. Two major incidents happened at 788.00 and 1096.00 m depths in the implementation process due to the very fragile strata, and to overcome the problems, two sidetracks (WFSD-3-S1 and WFSD-3-S2) were carried out. Therefore, WFSD-3, WFSD-3-S1, and WFSD-3-S2 reached 1186.77, 788.00–1187.28, and 1096.00–1502.3 m, respectively (Fig. 4a), with the core diameters ranging from 311 to 76 mm. The borehole dips to the SE-S at 88°–89° for depths of less than 400 m, dips to the S at 86°–88° for depth of 400–788 m, and dips to the S at 82°–86° for depths were greater than 788 m. A total of 1433.88 m of core was successfully retrieved from the surface to 1502.30 m depth, with a recovery of 92.54 %. In order to avoid disturbances, all cores were cataloged immediately after retrieval from the borehole, and detailed analyses were carried out in the laboratory afterward. Viewed from the temperature profile, the geothermal gradient of WFSD-3 is ~1.68 °C/100 m, which is much smaller than the ~2.15 °C/100 m gradient that was obtained from WFSD-1 (Li et al. 2014).

Results

Core description

Lithology and stratigraphy

The drill core of WFSD-3 appears mainly gray to dark-gray, and is composed of sandstone, siltstone, carbonaceous siltstone, liquefied breccia, coal seam, and fault breccia, as well as fault gouge (Fig. 5). Diagonal bedding along with plants and carbonaceous debris can be seen in the siltstone. Liquefied breccia is the product of soft-sediment deformation caused by paleoearthquakes (Qiao et al. 2012). Recent research results show that liquefied breccia was discovered in the middle (T_3x^2) and lower (T_3x^1) segments of the Xujiahe Formation (Qiao et al. 2012). Coal seams are also present in the WFSD-3 cores (Figs. 5, 6). Combined with regional stratigraphic characteristics, the cores mainly consist of the middle (T_3x^2) and upper (T_3x^3) segments of the Xujiahe Formation in a reversed sequence. Viewed from the lithological profiles (Fig. 6), the reversed sequence can be seen by the middle (T_3x^2) segment of the Xujiahe Formation above 260 m depth, and the upper (T_3x^3) segment of the Xujiahe Formation below 260 m depth.

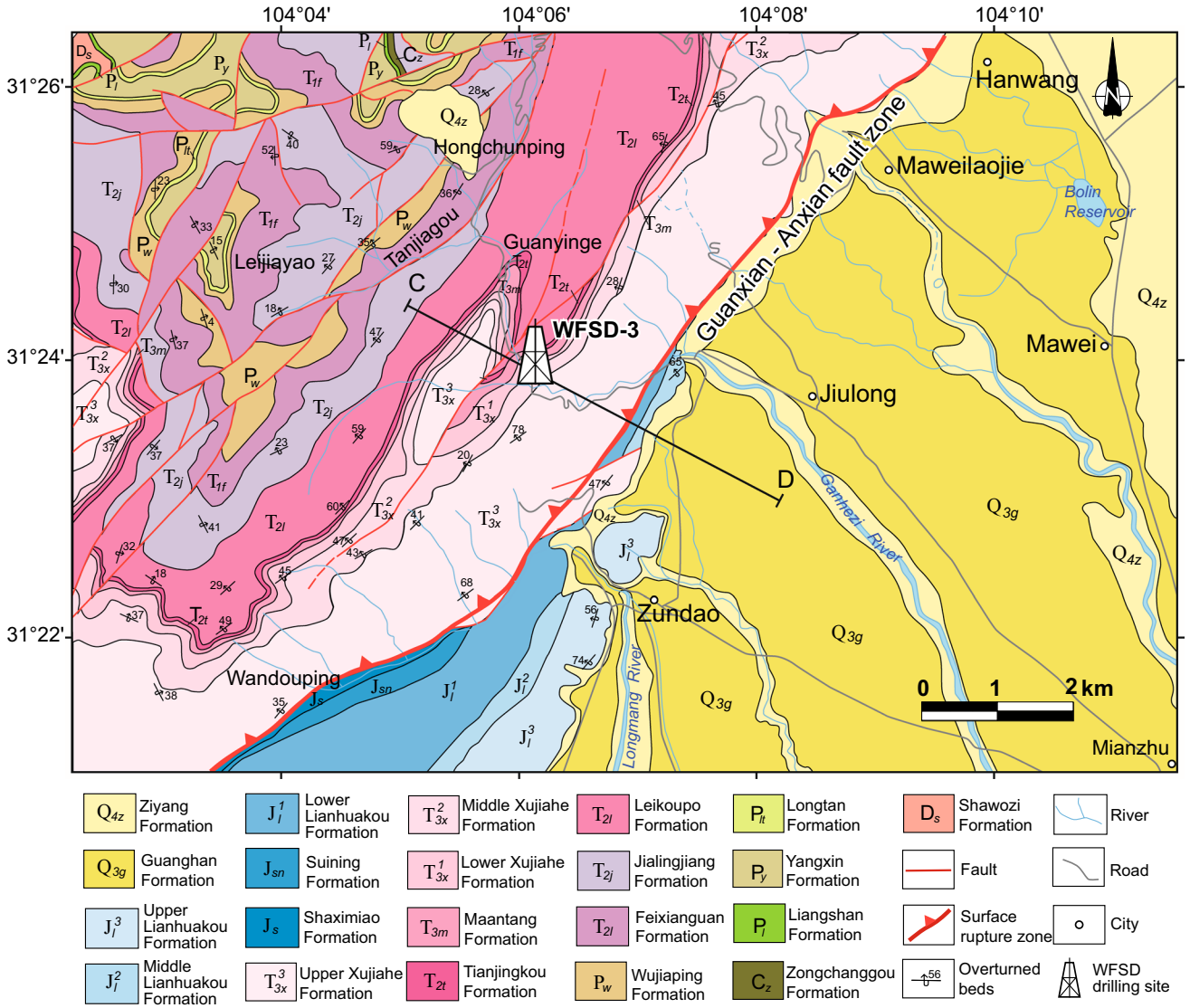

Fig. 3 Geological map of Jiulong area in Mianzhu, Sichuan (according to Sichuan Geology and Mineral Resources Bureau, geological map of Mianzhu area 1:50000, 1996), and WFSD-3 drilling site location. C–D profiles shown in Fig. 14

Fault-related rocks

The classification of the fault-related rocks in the WFSD-3 cores follows the textural classification of Sibson (1977), based on the rock structures and the volume fraction of visible rock fragments. Detailed observation and analyses show that fault gouge and fault breccia are visible in the WFSD-3 cores (Figs. 5, 6), while cataclasite and pseudotachylyte have not been found yet.

Fault gouge is visible in different lithologies (Fig. 6) with gray, dark-gray, and black appearance (Fig. 5). Fault gouge is foliated with a few small clasts which is completely different from the fault gouge in the WFSD-1 cores, where many more clasts of uneven size are observed (Li et al. 2013). Most of the fault gouge expanded rapidly right after being retrieved from the borehole; then, after a few days, fractures formed directionally in the gouge when water evaporated. In the WFSD-3 cores, the thicknesses of fault gouge vary from a few millimeters to meters. The thickest fault gouge is about 2.30 m (drilling thickness) at 1247.79–1250.09 m depth. Carbonaceous material can be seen in some fault gouge, which means the fault gouge might contain the original coal lines. Based on detailed statistics, coal seams are mostly distributed in or near the fault breccia and fault gouge, suggesting that coal seams might be related to fault activity. Fault breccia in the WFSD-3 cores is distinguished based on the volume fraction of visible clasts >30 %. Fractures are well developed in the WFSD-3 cores. The cores are mainly brittle above 1250 m depth with many fault rocks, and below that depth, the cores are more intact with much fewer fault rocks.

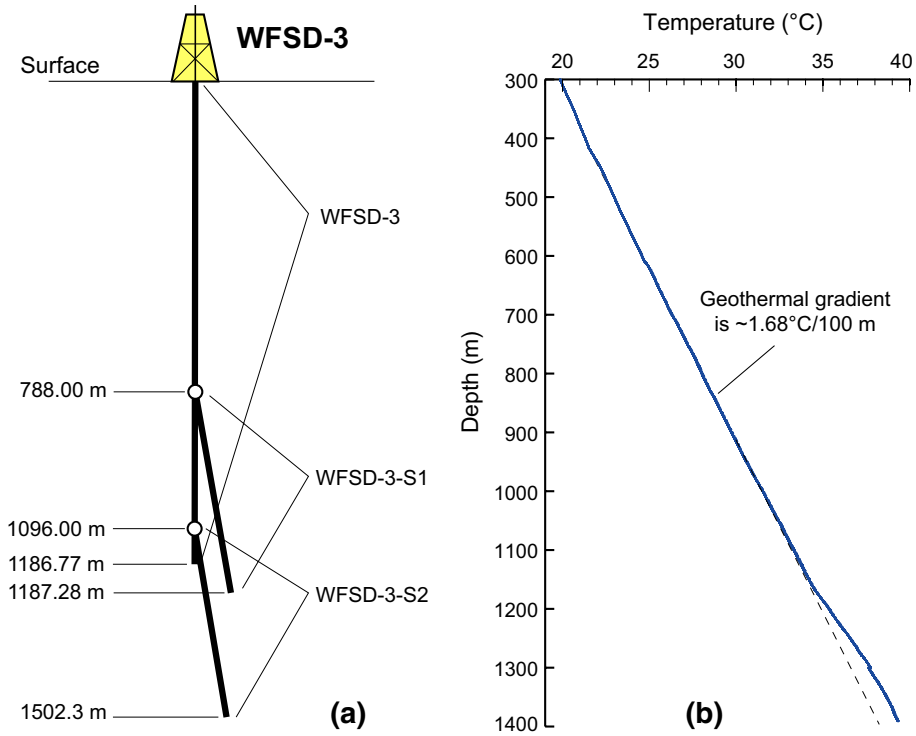

Fig. 4 **a** Drilling structure diagram of WFSD-3, the first sidetrack starts from 788 m depth and the second sidetrack starts from 1096 m depth; **b** Temperature profile of WFSD-3

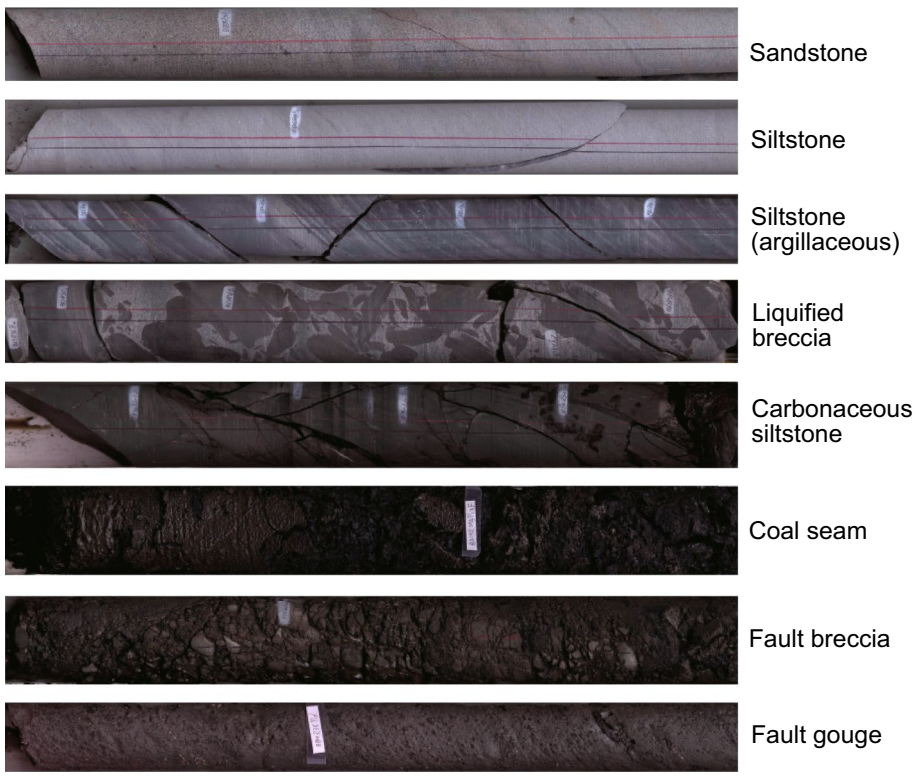

Fig. 5 Photographs of WFSD-3 cores with different lithology

Location of fault zones

The WFSD-3 cores contain many fault zones viewed from the distribution of fault rocks. The fault zones bear different fault rocks. Fault gouge, inferred to be the slip zones (cores of the fault zone), have thicknesses ranging from a few mm to 2.30 m. The fault zones have a cumulative gouge layer composed of many fault cores of subsidiary faults with thin

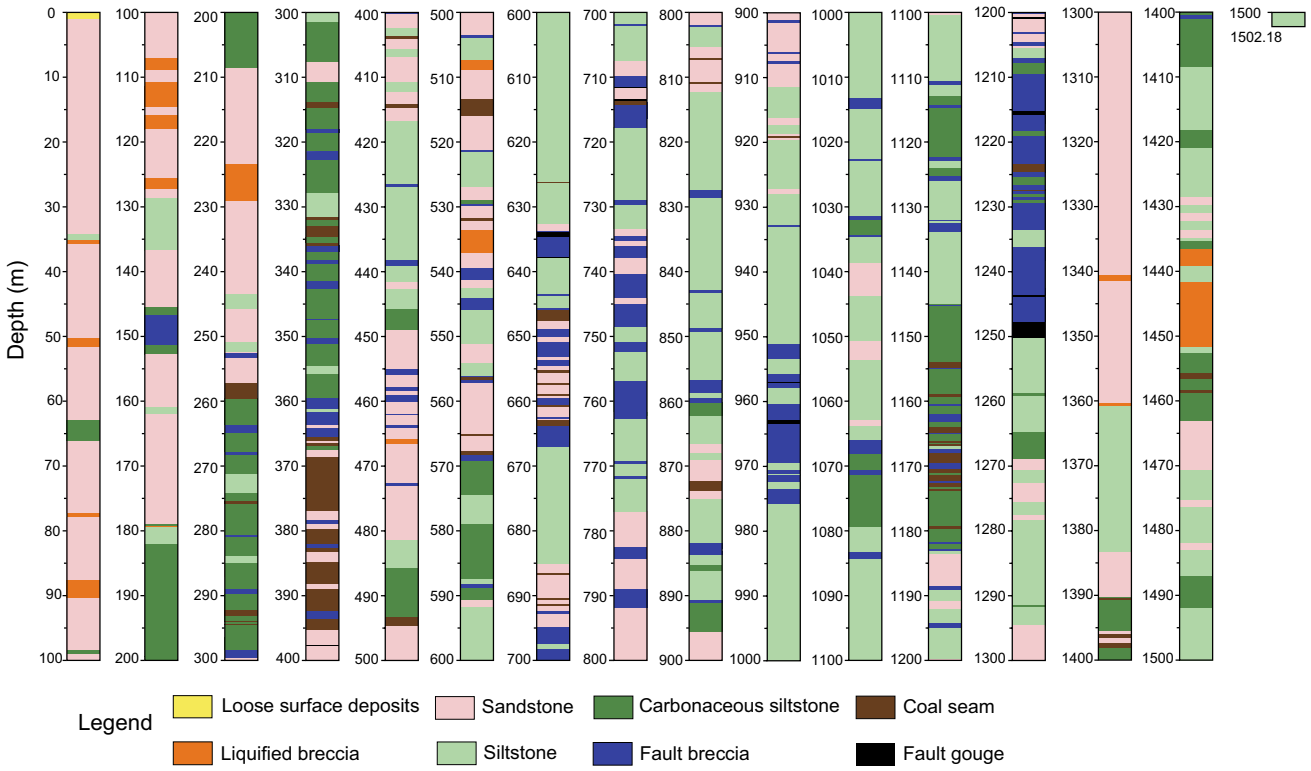

Fig. 6 Lithology chart and fault rock distributions along WFSD-3 cores, with depths being the borehole depths

gouge layers. To obtain the actual widths and thicknesses of the gouge mentioned above, the values should be multiplied by cos θ (where θ is the dip angle of the borehole).

In order to show the distribution of fault zones more clearly, fault density of the WFSD-3 cores was calculated (see detailed calculation method in Li et al. 2013). As shown in Fig. 7, 22 fault zones (cores) are recognized. According to the logging data and the core measurements, most of these fault zones trend to the NW with dip angles of 40°–60°, and the dip angles gradually decrease from the top to the bottom. There are four major fault zones: FZ634 (fault zone at 634 m depth), FZ963, FZ1215, and FZ1250. The thickness of the gouge in these four fault zones is far larger than the others, yielding a higher fault density as well (Fig. 7).

The thickness of the FZ634 fault zone is 4.04 m from 633.87 to 637.91 m depth, and is composed of fault breccia and fault gouge (Fig. 8a). The fault breccia is 0.67 m thick with a 0.22-m foliated layer. The fault gouge is 0.85 m thick and is located at depths of 33.87–634.50 and 637.69–637.91 m where foliation is developed. The protolith of the fault rocks is argillaceous siltstone, similar to the wall rock.

The FZ963 fault zone is 9.15 m thick, located at 960.3–969.45 m depth, and is composed of fault breccia and fault gouge (Fig. 8b). Foliation is present in the 0.68-m-thick fault gouge (962.89–963.57 m). Fault breccia is ~8.47 m thick. The protolith of the fault rocks is argillaceous siltstone.

The FZ1215 fault zone lies at depths of 1209.5–1223.45 m, is 13.95 m thick, and is composed of fault breccia and fault gouge (Fig. 8c). Foliation is visible in the 0.72-m-thick fault gouge (1215.07–1215.79 m). Fault breccia is ~12.14 m thick. The protolith of the fault rocks is argillaceous siltstone.

The FZ1250 fault zone is located at depths of 1236.18–1250.09 m, with a thickness of 13.91 m. It consists of fault breccia and fault gouge (Fig. 8d). The fault breccia is 10.73 m thick with a 0.63-m foliated zone. The fault gouge is 2.55 m thick and is distributed at depths of 1236.88–1237.04, 1242.52–1242.56, 1243.87–1243.92, and 1247.79–1250.09 m. Foliation is visible in the fault gouge.

Logging data

The logging of the WFSD-3 borehole was undertaken by Shengli Well Logging Company of the Sinopec Group and the Institute of Geophysical and Geochemical Exploration, Chinese Academy of Geological Sciences (CAGS). Five comprehensive logging sets were conducted in total. The logging depths of the first three measurements were 23.74–409.66, 407.5–1144, and 1100–1186.77 m, respectively, with borehole diameters of ≥150 mm. The instruments

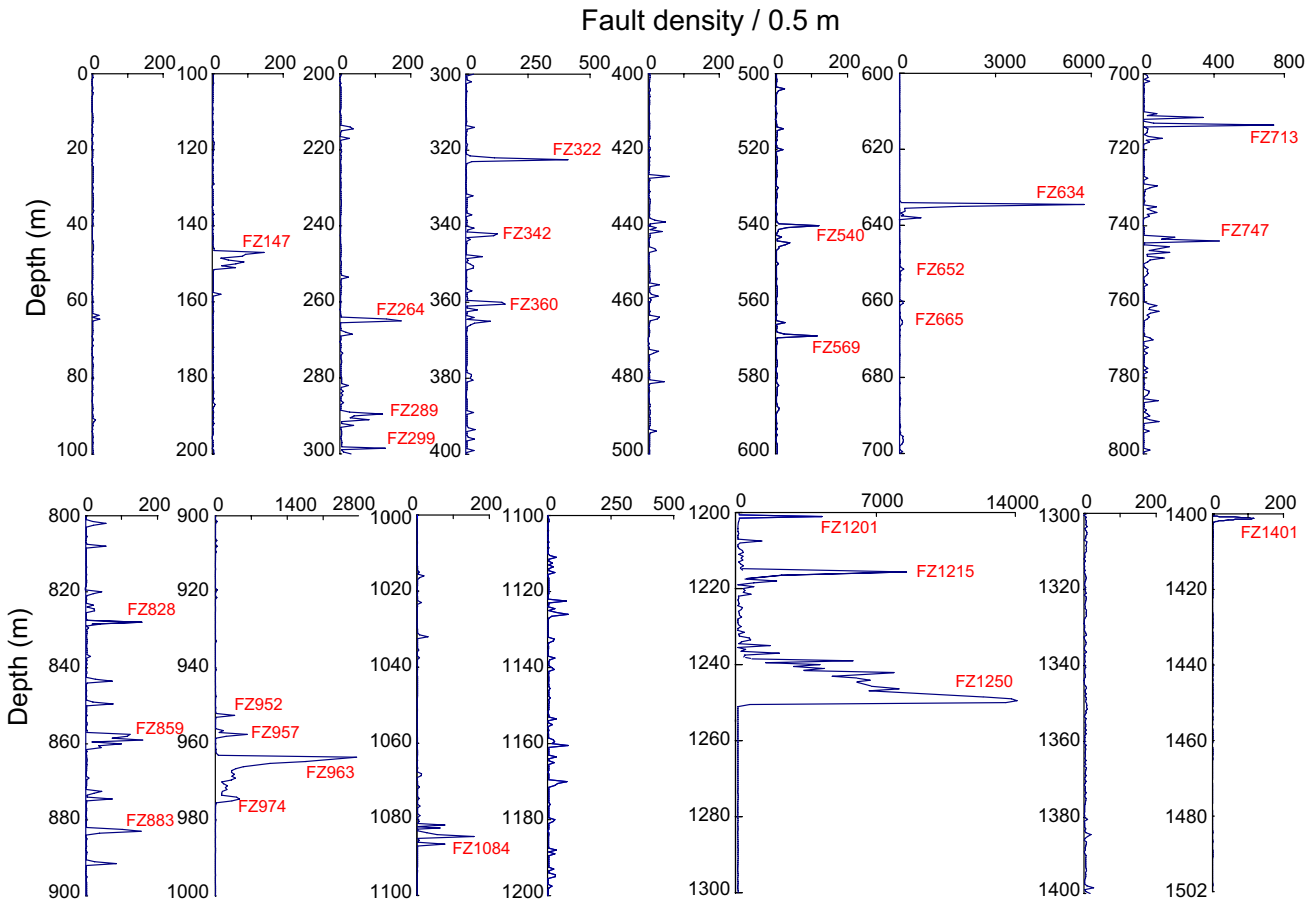

Fig. 7 Distribution of fault density profile of WFSD-3 cores. There are many fault zones (cores) in the WFSD-3 cores. To determine their activity, different peaks represent different fault (cores) densities. See Li et al. (2013) for details

used for the first three measurements were an Eclips-5700 of SDL-ATLAS and an Excell-2000 imaging logging of Halliburton. A Shengli 6000 (Φ76) of the Shengli Logging Company was used for the fourth survey at depths of 1180.66–1404.53 m, where the borehole diameter was ~100 mm. Electric and acoustic imaging logging data were not obtained due to the small borehole diameter and high drilling fluid density. The logging depth of the fifth survey was 1404.5–1501.5 m with a borehole diameter of ~76 mm, carried out by the Institute of Geophysical and Geochemical Exploration, using a Micrologger II of the RG Logging CO., LTD, and JGS-1B produced by the Chongqing Geological Instrument Factory.

Viewed from the curves in Fig. 9, the borehole diameter largely expanded at depths of 143–305, 695–775, 820–835, and 948–975 m. The relationship between natural gamma ray and lithologies is obvious. The natural gamma ray values for medium- to fine-grained sandstone is lower at about 40–60 API, and for mudstone, it is higher at about 130–150 API. The natural gamma ray values increase with the content of argillaceous materials from sandstone, siltstone, pelitic siltstone, and silty mudstone to mudstone. The deep lateral apparent resistivity decreases from 1400 to 20 Ωm at depths increasing from 40 to 1250 m. The density values are less than 2.0 g/cm^3 at various depths along the density curve, which might indicate coal-bearing strata or coal seams, besides the influence of the borehole diameter. The apparent neutron porosity of sandy argillaceous increases with the argillaceous content and rock porosity. The mid-value of this section is 17.70 (Table 1) and is equivalent to the apparent neutron porosity of argillaceous siltstone. High values of acoustic time visible in the curves may indicate coal seams, gouge, and damage zone, assuming that the change in borehole diameter can be ignored.

It is difficult to distinguish the coal seams from other rocks in the Xujiahe Formation using physical properties, such as natural gamma and electrical resistivity. Coal density is commonly 1.3–1.4 g/cm^3, while the densities of the other rocks are usually greater than 2.2 g/cm^3. Therefore, except for the clear increase due to the change in the borehole diameter, a density less than 2 g/cm^3 can be considered

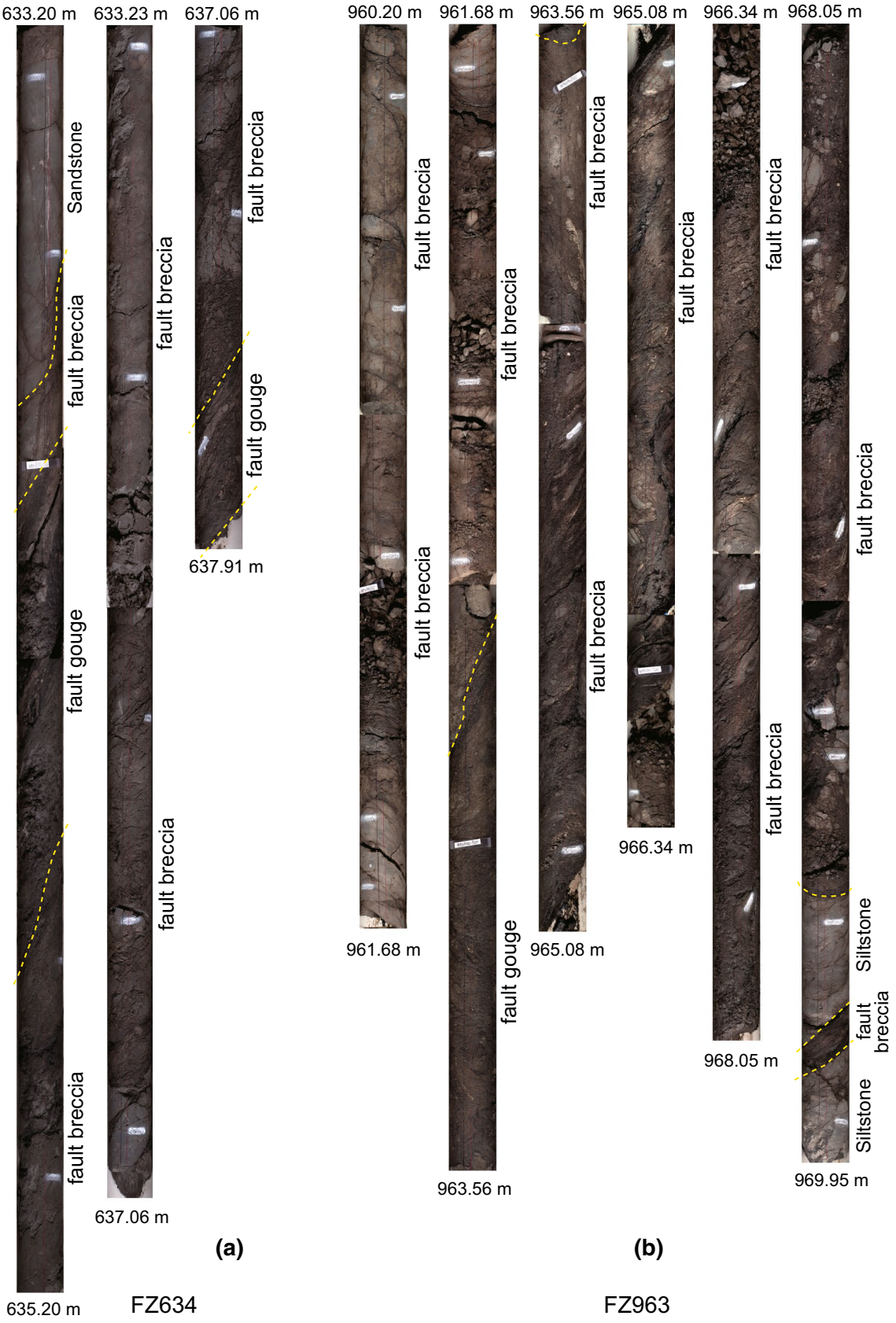

Fig. 8 Photographs of the major fault zones in the WFSD-3 cores. **a** FZ634, **b** FZ963, **c** FZ1215, and **d** FZ1250

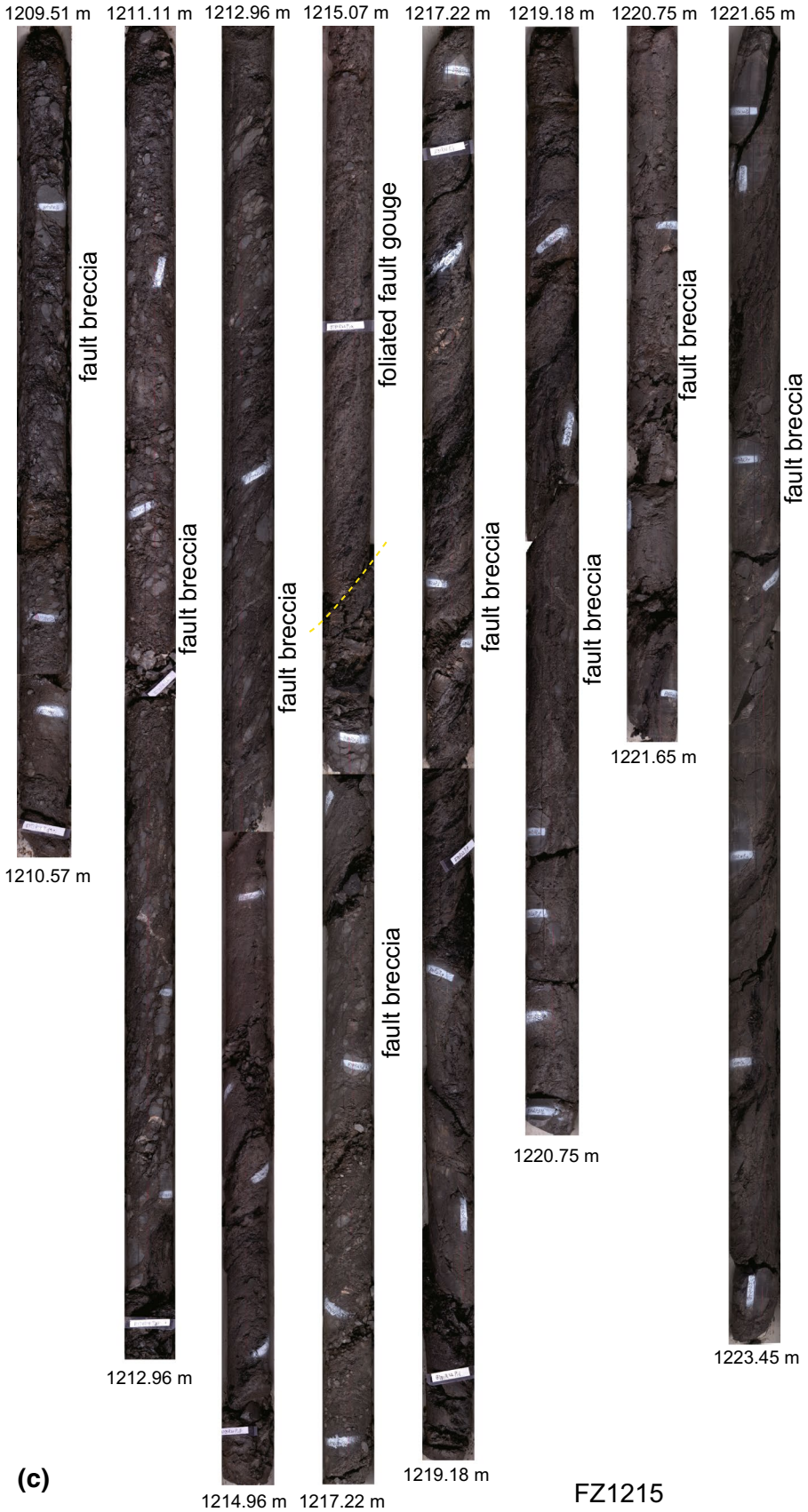

Fig. 8 continued

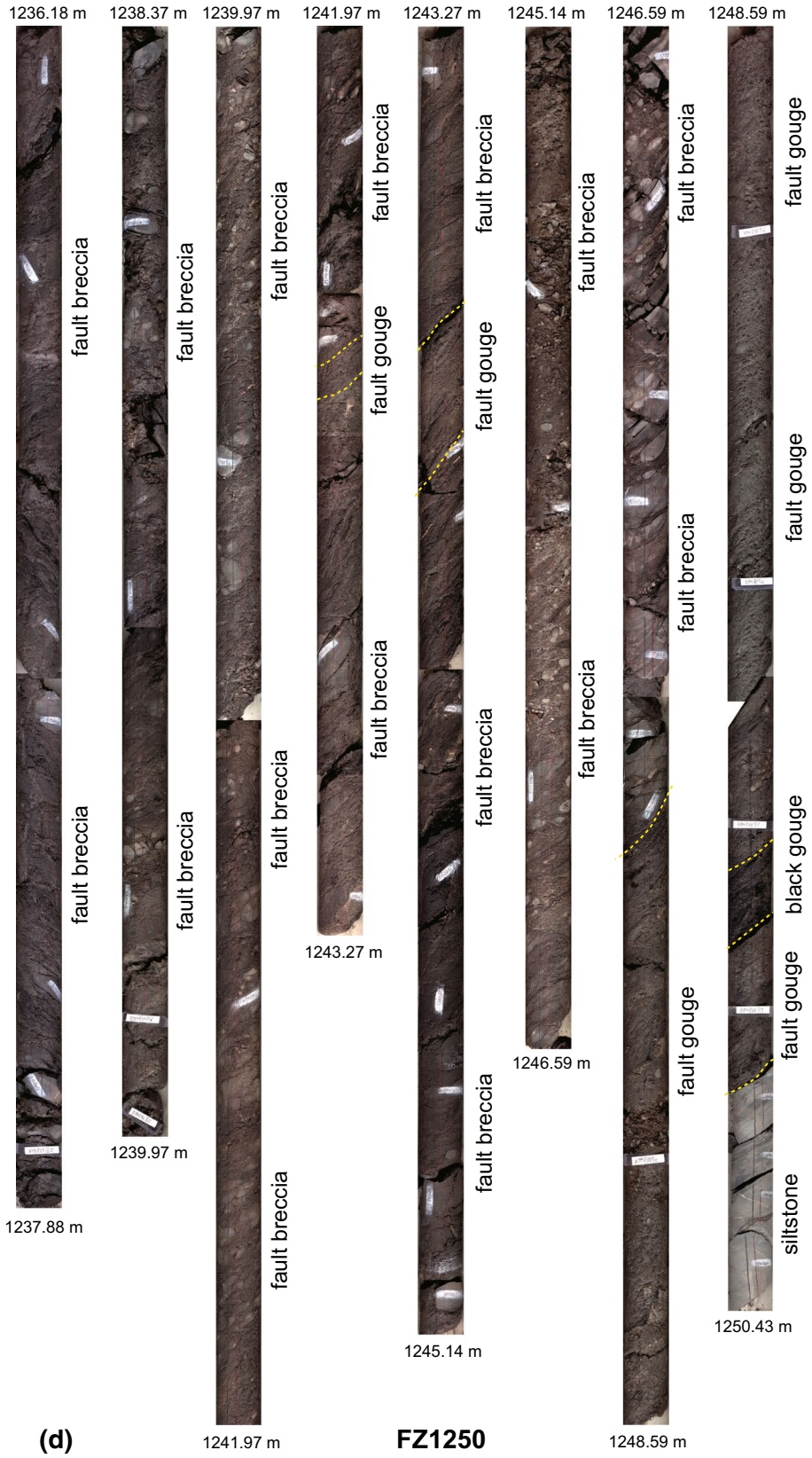

Fig. 8 continued

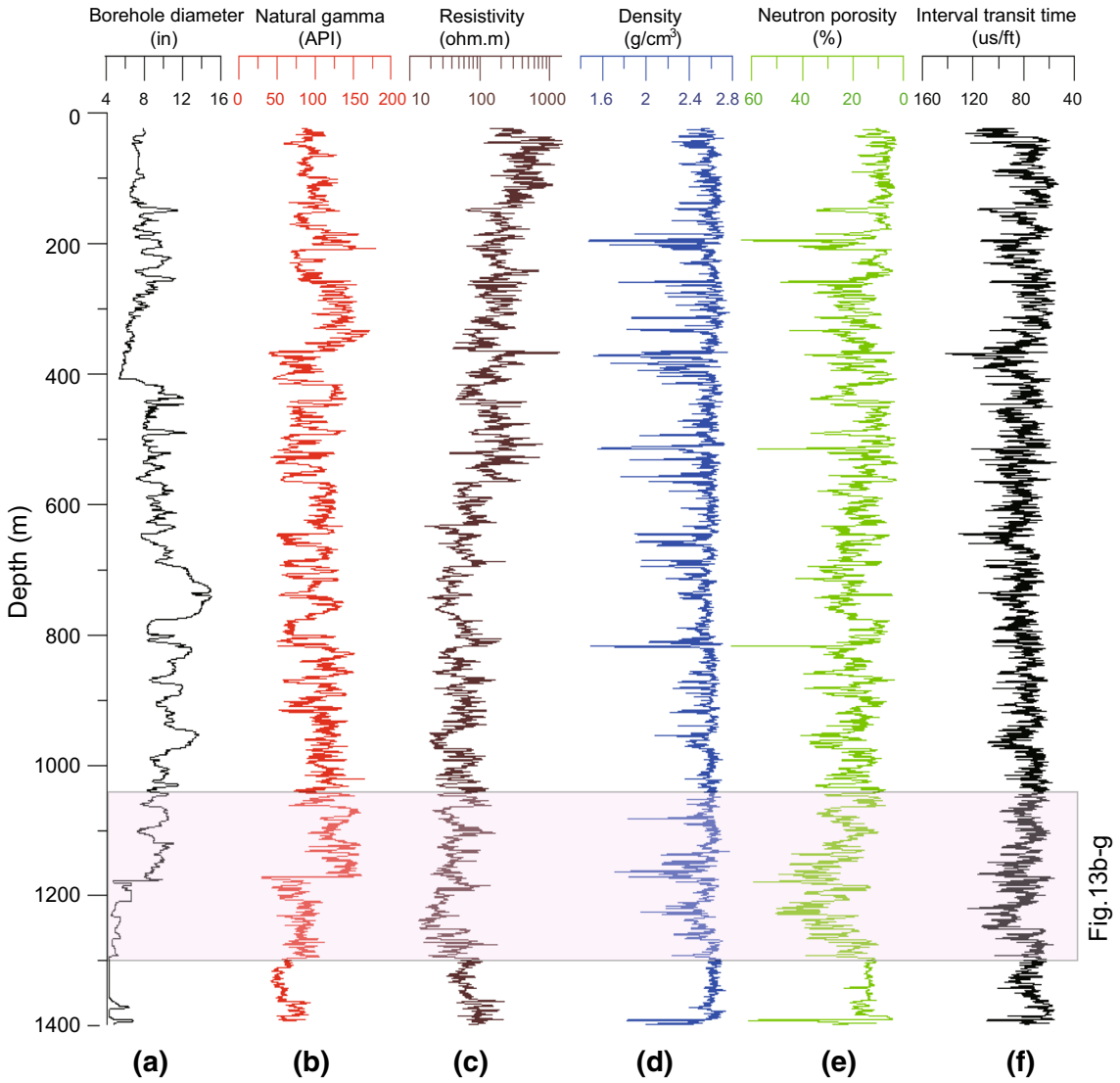

Fig. 9 Logging data from 24 to 1400 m depth in WFSD-3 borehole. (*a*) Borehole diameter; (*b*) Natural gamma; (*c*) Deep lateral resistivity; (*d*) Density; (*e*) Neutron porosity; (*f*) Interval transit time (inversely proportional to the wave velocity)

Table 1 Main logging parameters in WFSD-3 (24–1400 m)

Logging parameters	Natural gamma (API)	Density (g/cm^3)	Apparent resistivity (Ω m)	Interval transit time (μs/ft)	Apparent neutron porosity (%)	Photoelectric index (b e^{-1})
Maximum	178.68	2.76	1456.19	142.47	68.43	7.81
Minimum	28.04	1.46	13.03	53.79	3.02	1.01
Average value	98.12	2.53	126.88	79.91	18.78	2.95
Mid-value	98.57	2.58	71.99	78.49	17.70	2.95
Standard deviation	26.99	0.15	150.74	12.02	8.91	0.67

as coal-bearing strata and a density less than 1.8 g/cm^3 can be considered as coal seam (Fig. 10).

The borehole diameter, natural gamma, neutron porosity, and acoustic time increase in a typical damage zone or fault zone, while the electrical resistivity and density decrease (Li et al. 2014). Based on the logging data, 16 fault zones were recognized (Table 2), while the major fault zones are at depths of 145–165, 216–238, 641–664, 1205–1229, and

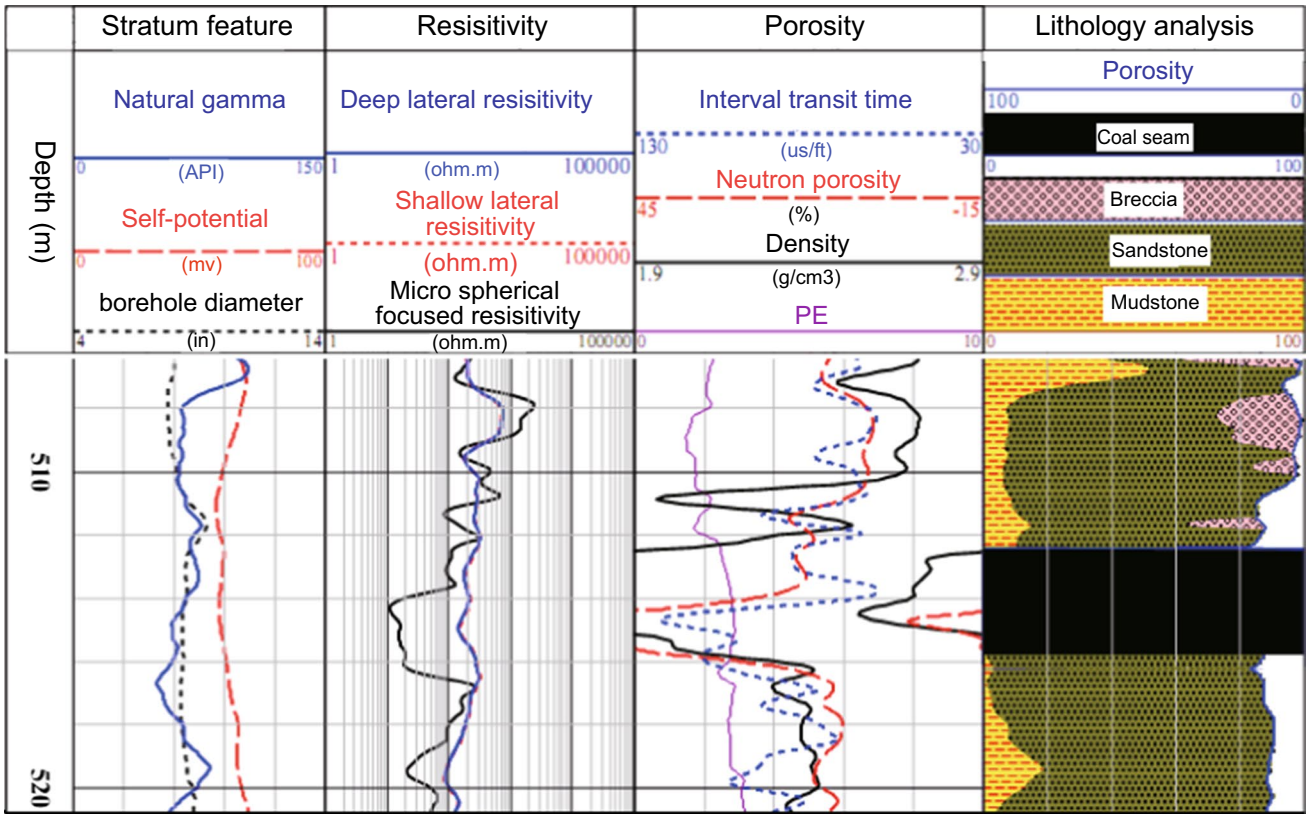

Fig. 10 Logging data response of coal seam from 512.4 to 515.2 m depth in WFSD-3

Table 2 Characteristics of the fault rock zones/cores in the WFSD-3 cores

Sequence number	Top depth (m)	Bottom depth (m)	Thickness (m)
1	145	165	20
2	216	238	22
3	260	272	12
4	356	365	9
5	378	383	5
6	531	541	10
7	564	570	6
8	641	664	23
9	740	746	6
10	820	830	10
11	954	964	10
12	1081	1091	10
13	1149	1166	17
14	1205	1229	24
15	1236	1250.09	24
16	1400	1401	1

1236–1250.09 m, which is similar to the fault zone distribution estimated by characteristics of the fault rocks in the WFSD-3 cores.

Discussion

Fractures and fault zone distributions as well as stress field analysis in WFSD-3 borehole

The fault zones and fractures in the WFSD-3 are mainly caused by tectonic stress that can reflect the state of the stress field in the Longmen Shan area. Based on the resistivity and ultrasonic imaging logging data, together with the cores, fracture characteristics were analyzed. The results show that fractures are developed in the WFSD-3 cores, especially at depths of 25–200 and 900–1000 m (Fig. 11). The dip angles of the fractures range from 10° to 80°, mostly between 60° and 70°. The fracture patterns vary at different depths: depths of 25–410 m depth dips toward N260°–290°E at 30°–80° (mostly 40°–50°); 410–730 m depth dips toward N330°–360°E with dip angle of 30°–80° (mostly 60°–70°); depths of 730–960 m depth dips to N210°–240°E at 30°–80° (mostly 60°–70°); 960–1185 m depth dips toward N260°–290°E at 30°–80° (similar to the 24–410 m depth range); for 1410–1450 m depth, trends mainly N180°–200°E. Fractures are closely related to the fault zones and beddings, which are controlled by the tectonic features.

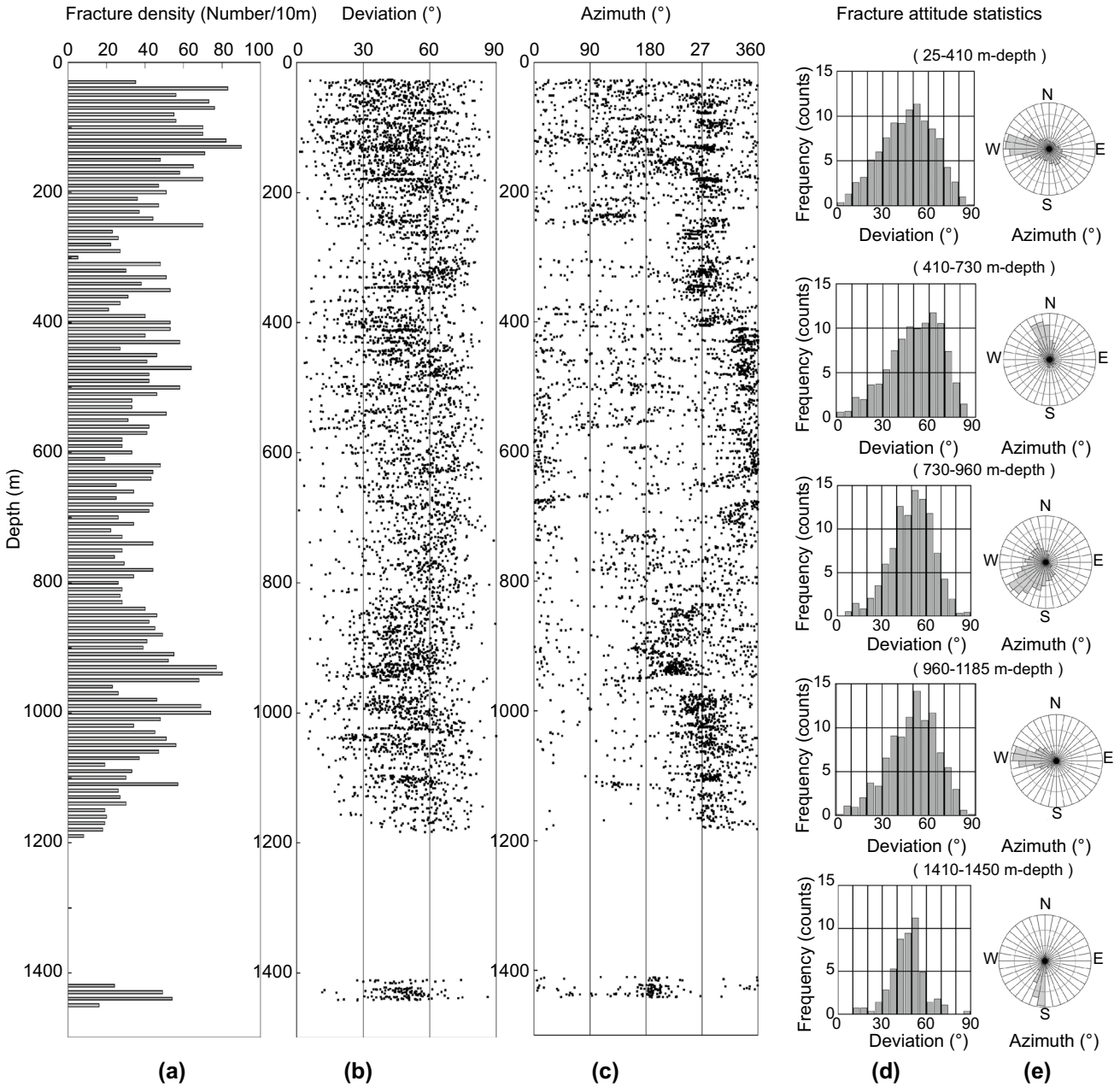

Fig. 11 Fracture distribution characteristics in WFSD-3 borehole. **a** Fracture density; **b** Dip angle of fracture; **c** Dip direction of fracture; **d** Dip angle trend; **e** Dip direction trend

Electric and acoustic imaging logging data were not obtained during the fourth logging at depths of 1180.66–1404.53 m due to the small borehole diameter and high drilling fluid density. Therefore, the distribution of fractures and faults at these depths cannot be seen in the logging data. However, we can speculate about the rock properties based on the continuity of WFSD-3 cores and their simple structures.

According to the analysis of logging data and fracture characteristics of the cores, the major faults FZ634, FZ963, FZ1215, and FZ1250 dip to N342°E at ~52°, N220°–250°E at ~48°, N240°–260°E at ~41°, and N270°–290°E at ~38°, respectively. Based on the analyses of fracture occurrences (Fig. 11) and fault zone distributions, the azimuth of the stress field varies with depth: For 25–410 m depth, the maximum principal stress is mainly oriented WNW–ESE; for 410–730 m depth, it is mainly NW–SE; for 730–960 m depth, it is SW–NE; for 960–1250 m depth, it is WNW–ESE; and for 1410–1450 m depth, it is N–S. These speculated stress field azimuths represent a complicated pattern

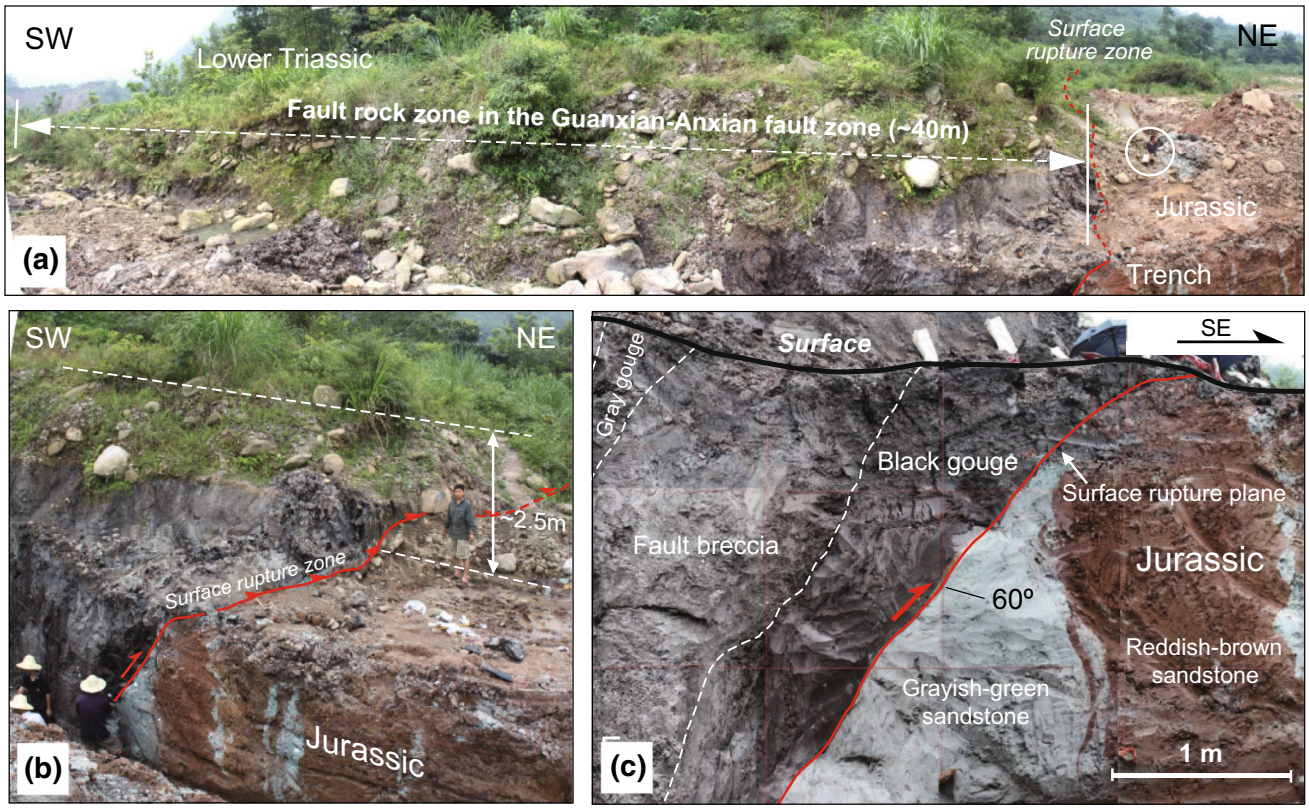

Fig. 12 Photographs of outcrops of the Guanxian–Anxian fault zone at Qingquan village, Jiulong county (see Fig. 3 for the location). **a** Surface outcrop of the fault zone along the north side of the river; **b** Surface rupture zone showing vertical offsets of ~2.5 m, the trench across the surface rupture zone; **c** The north wall of the trench

which cannot represent the current stress field azimuth, because the fracture statistics include the fractures formed at different periods by different mechanisms. However, the stress field azimuths for depths of active faulting less than 1250 m are obviously different from that for depths greater than 1410 m.

Structure and width of the Guanxian–Anxian fault zone

A fault zone is usually composed of a fault core and a damage zone (Spray 1995; Sibson 1977; Faulkner et al. 2010; Gudmundsson 2011). The fault core is generally composed of fault gouge, fault breccia, cataclasite or ultracataclasite (or a combination of both), while the damage zone is generally composed of fractures over a wide range of length scales and subsidiary faults. Some faults may have a single high-strain fault core (Chester and Logan 1986), and others might be a combination of fracture zones with multiple high-strain fault cores (Faulkner and Rutter 2003). The Yingxiu–Beichuan fault zone is a combined fault zone with multiple high-strain fault cores (Li et al. 2013; Wang et al. 2014).

The Wenchuan earthquake caused a ~80-km-long coseismic surface rupture zone along the Guanxian–Anxian fault. Field investigation shows that the surface rupture zone strikes N10°E and dips to the west, crosses the riverbed, and produces a maximum vertical offset of 4.2 m (Li et al. 2008) in Qingquan village, Jiulong county, Mianzhu city. A 10-m-long, 3-m-deep, and 2.5-m-wide trench was excavated across the rupture zone at that location (Fig. 12) (Liu et al. 2014). The Wenchuan earthquake slip zone is sharp and dips to the NW with a dip angle of 60°, which is clearly visible in the trench profile (Fig. 12). On the east side of the slip plane, it is grayish-green and reddish-brown Jurassic sandstone with little or no fractures. On the west side, there are ~1.0-m-thick foliated black fault gouge and ~0.5-m-thick gray fault gouge, as well as some fault breccias with oriented structures. There is a clear asymmetrical fault zone structure, i.e., fault gouge, fault breccia, and/or fractures only developed in the hanging wall. This result is similar to the Nojima fault zone in Japan which shows asymmetrical characteristics with fracture zones only found in the hanging wall (Lin et al. 2007). Viewed from the surface outcrop, the Guanxian–Anxian fault zone is composed of multilayer foliated black gouge with a cumulative

thickness of ≥3 m, fault breccia ≥30 m with oriented/weakly oriented structures, and several meters of non-oriented breccia. Therefore, the width of the fault rocks (fault core) of the Guanxian–Anxian fault zone exposed at the outcrop is at least 40 m (Fig. 12). The exact width of the damage zone is not clear due to the lush vegetation, but at least a 100 m width can be tracked. The damage zone is only present on the west side of the fault rock zones along the hanging wall, again showing that the Guanxian–Anxian fault zone has an asymmetrical fault structure.

The major fault zone is composed of many small-scale subsidiary fault zones. 22 small fault zones are recognized in WFSD-3 cores. A single subsidiary fault zone is composed of fault gouge, fault breccia, and damaged wall rocks. The fault gouge has various thicknesses of a few millimeters to several meters. Viewed from the fault rock distributions in WFSD-3 cores (Fig. 6), a continuous fault zone is seen from 1200 to 1250.09 m depth, where the black fault gouges are present at depths of 1201, 1215.07–1215.79, 1236.88–1237.04, 1242.52–1242.56, 1243.87–1243.92, and 1247.79–1250.09 m, while fault breccia are mainly interlayered between the fault gouge layers. Therefore, we consider the combination of the small subsidiary fault zones as the major fault zone. This is similar to the observation from the surface outcrop, indicating that the Guanxian–Anxian fault zone has characteristics of a multiple core model. In addition, according to the logging data, the electrical resistivity at depths of 1192–1250.09 m is lower than other sections (Fig. 9). For these reasons, we conclude that this is the major fault zone of the Guanxian–Anxian fault zone, which is composed of at least 60-m-thick fault rocks in WFSD-3 cores, The actual width is ~50 m taking into account the dip. The average trend of foliations is N264°E, and the average dip angle is 40°.

According to the logging data and lithology profile of WFSD-3, rock fractures are abundant at depths less than 1250.09 m which can be used to identify the damage zone of the Guanxian–Anxian fault zone. Viewed in Fig. 11, from 980 to 1200 m depth, the occurrences of fractures mostly dip to the west with angles of 30°–60°, which is consistent with that of the fault rocks at 1192–1250.09 m depth. Also, there is a boundary of fracture density at ~980 m depth (Fig. 11). Therefore, we infer that the actual width of the damage zone of the Guanxian–Anxian fault zone is ~160 m (from ~980 to 1200 m depth in WFSD-3 cores). Then, the total thickness of the Guanxian–Anxian fault zone is ~210 m (~50 m fault rocks and ~160 m damage zone).

The principal slip zone (PSZ) of the Wenchuan earthquake in WFSD-3 cores

Identifying the PSZ that ruptured in the Wenchuan earthquake is important for studying the fault mechanism, physical–chemical changes in the rocks, as well as the long-time monitoring on the seismic, temperature, fluids, and stress field after the borehole drilling was completed. Therefore, it is of great importance to locate the PSZ of the Wenchuan earthquake in the WFSD-3 cores.

According to previous research, the PSZ is located at the fault core (fault gouge) (Sibson 2003; Ma et al. 2006; Song et al. 2007; Kuo et al. 2009, 2011; Li et al. 2013, 2014; Wang et al. 2014). There are 22 fault zones in the WFSD-3 cores, and each has multilayers of fault gouge. Which is the coseismic fault of the Wenchuan earthquake? Which layer of fault gouge represents the PSZ? A ~80-km-long surface rupture along the Guanxian–Anxian fault is the boundary between the Late Triassic Xujiahe Formation and the Jurassic strata in the studied area. The fault zone is at least 40 m wide viewed from the outcrop at Qingquan village, Jiulong county (Fig. 12). For the surface fault, the coseismic rupture zone is seen at the bottom of the fault zone. In the excavated trench, the coseismic slip plane is clearly located at the boundary of the black gouge, directly in contact with the undeformed Jurassic sandstone in the footwall (Fig. 12).

In the WFSD-3 cores, only below FZ1250, the rocks are intact with few fractures, and the black gouge at 1247.79–1250.09 m depth is directly overlying the undeformed gray sandstone (Figs. 6, 8d), which is similar to that observed from the outcrop. Therefore, by comparison to the outcrop observations, we consider that the PSZ is likely located in this fault gouge layer.

Only several mm to 2 cm or even thinner fault gouge can be produced by one large earthquake (Ma et al. 2006; Kuo et al. 2009, 2014; Li et al. 2013). It is difficult to identify the exact PSZ location in the ~2.3-m-thick fault gouge in WFSD-3 cores, but we can tentatively determine its location based on the appearance of the fault gouge. Thin fresh fault gouge and cracking near the sliding surface has been found in the PSZ of the Wenchuan earthquake (Mw 7.9) in WFSD-1 (Li et al. 2013, 2014; Si et al. 2014), and similarly for the PSZ of the Chi–Chi earthquake (Mw 7.6) in the Taiwan Chelungpu fault Drilling Project (TCDP) (Ma et al. 2006; Kuo et al. 2009). Thus, the PSZ of the Wenchuan earthquake in the WFSD-3 cores is most likely in the black gouge at 1248.59–1250 m depth (Figs. 8d, 13).

Frictional temperature anomalies resulting from the earthquakes can be resolved in the vicinity of the seismogenic fault at depths (Brodsky et al. 2009). Rapid drilling after large earthquake provides an opportunity to measure the temperature anomalies near the slip planes (Kano et al. 2006; Fulton et al. 2013; Li et al. 2013). The temperature profile of the WFSD-3 borehole (Fig. 4b) shows that a positive temperature anomaly appears from the depth of ~1200 m, which probably indicates the residual frictional heat of the Wenchuan earthquake, although the anomaly

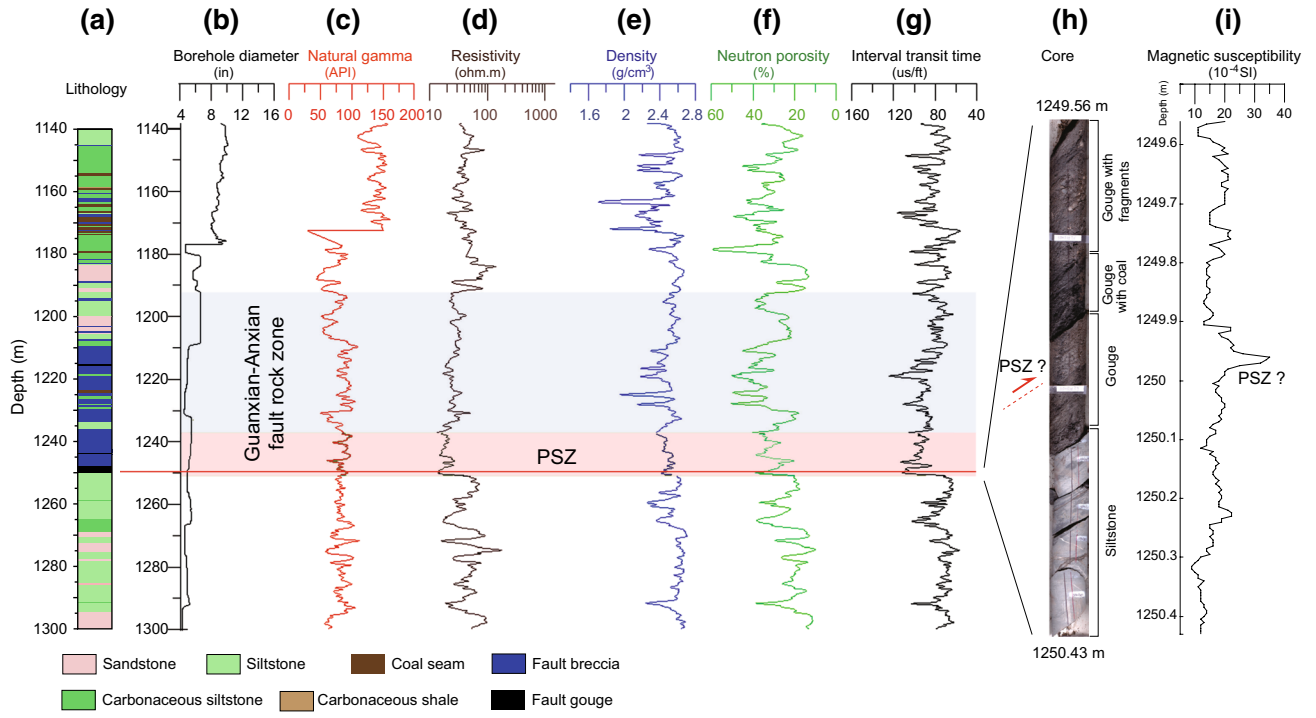

Fig. 13 Main fault zone logging response curve at 1140–1300 m deep in WFSD-3. At 1236–1250.09 m depth (*pink band*) has the lowest apparent resistivity in whole borehole. The *red line* shows the PSZ of the Wenchuan earthquake. (*a*) Lithological column; (*b*) Borehole diameter; (*c*) Natural gamma; (*d*) Deep lateral resistivity; (*e*) Density; (*f*) Neutron porosity; (*g*) Interval transit time (inversely proportional to the wave velocity); (*h*) Photograph of cores from 1249.56 to 1250.43 m; (*i*) Magnetic susceptibility

Table 3 Logging parameter statistics of the Wenchuan earthquake PSZ speculated in WFSD-3 (1140–1300 m)

Logging parameters	Natural gamma (API)	Density (g/cm3)	Apparent resistivity (Ω m)	Interval transit time (μs/ft)	Apparent neutron porosity (%)	Borehole diameter (in)
Maximum	99.15	2.56	26.14	113.72	40.79	5.34
Minimum	59.12	2.35	13.03	83.33	20.76	4.80
Average value	84.52	2.46	18.10	96.15	31.70	5.19
Mid-value	84.89	2.46	17.74	94.99	31.49	5.27
Standard deviation	8.12	0.05	3.14	7.68	4.33	0.16

width is very large. These thermal data also indicate that the PSZ of the Wenchuan earthquake is likely located in the fault gouge in FZ1250.

Previous research shows that PSZs are generally characterized by high magnetic susceptibility, low density, high porosity, low resistivity, high natural gamma ray, and low sound wave velocity (Li et al. 2013, 2014). Viewed from the logging data in the WFSD-3 borehole (Figs. 9, 13), the deep lateral resistivity at 1236–1250.09 m depth is less than 20 Ωm with a mid-value of 17.74 Ωm (the lowest value for the whole borehole). For 1236–1250.09 m depth, the natural gamma value is low with a mid-value of 84.89 API, mainly related to the fault gouge. The acoustic velocities (mid-value of 94.99 us/ft), neutron porosity (mid-value of 31.49 %), and density (mid-value of 2.46 g/cm^3) (Table 3) all show changes that may be indicative of the PSZ of the Wenchuan earthquake for this depth, but unfortunately, there are no imaging logging data to confirm this.

There are at least four layers of fault gouge in the FZ1250, but only one has the lowest apparent resistivity and higher magnetic susceptibility (Fig. 13) at ~1249.95 m depth. High magnetic susceptibility in the fault gouge may be due to the increase in magnetic mineral content caused by high-temperature frictional heating (Kano et al. 2006; Hirono et al. 2008; Pei et al. 2010; Liu et al. 2014). Only 1-mm to <2-cm-thick fault gouge is usually produced in a single earthquake, as seen in the Chi–Chi earthquake (Ma et al. 2006; Kuo et al. 2011, 2014), and the Wenchuan

earthquake in the WFSD-1 cores in the Yingxiu–Beichuan fault (Li et al. 2013; Si et al. 2014); therefore, the entire ~2–3-cm-thick fault gouge found here may have not been generated by the Wenchuan earthquake.

In summary, the geological and fault structure characteristics, observed both by the surface outcrop and the WFSD-3 cores, as well as the logging data, indicate that the PSZ of the Wenchuan earthquake is likely located in the black fault gouge at 1249.95 m depth in FZ1250. Connecting this with the surface outcrop, this result indicates that the dip angle of the coseismic slip plane in the WFSD-3 hole is 38°, confirming that it is a low-angle thrust fault. The dip angle is less than the value of 58° obtained by the focal mechanisms of the aftershocks of the Wenchuan earthquake (Yu et al. 2010), also it is somewhat different from the value obtained from seismic reflection profiles (Lu et al. 2012).

Wenchuan earthquake fault structures

The Wenchuan earthquake fault zone includes the Yingxiu–Beichuan and the Guanxian–Anxian fault zones. Results from the WFSD-1 cores and surface outcrop (Li et al. 2013; Wang et al. 2014, 2015) show that the Yingxiu–Beichuan fault zone is about 200 m wide (thickness of the fault rocks) with individual fault gouge thicknesses ranging from 2 mm to ~4 m. The fault that ruptured during the Wenchuan earthquake along the Yingxiu–Beichuan fault zone is a high-angle thrust fault with a dip angle of 75°–65° from the surface to 600 m depth. For that fault segment,

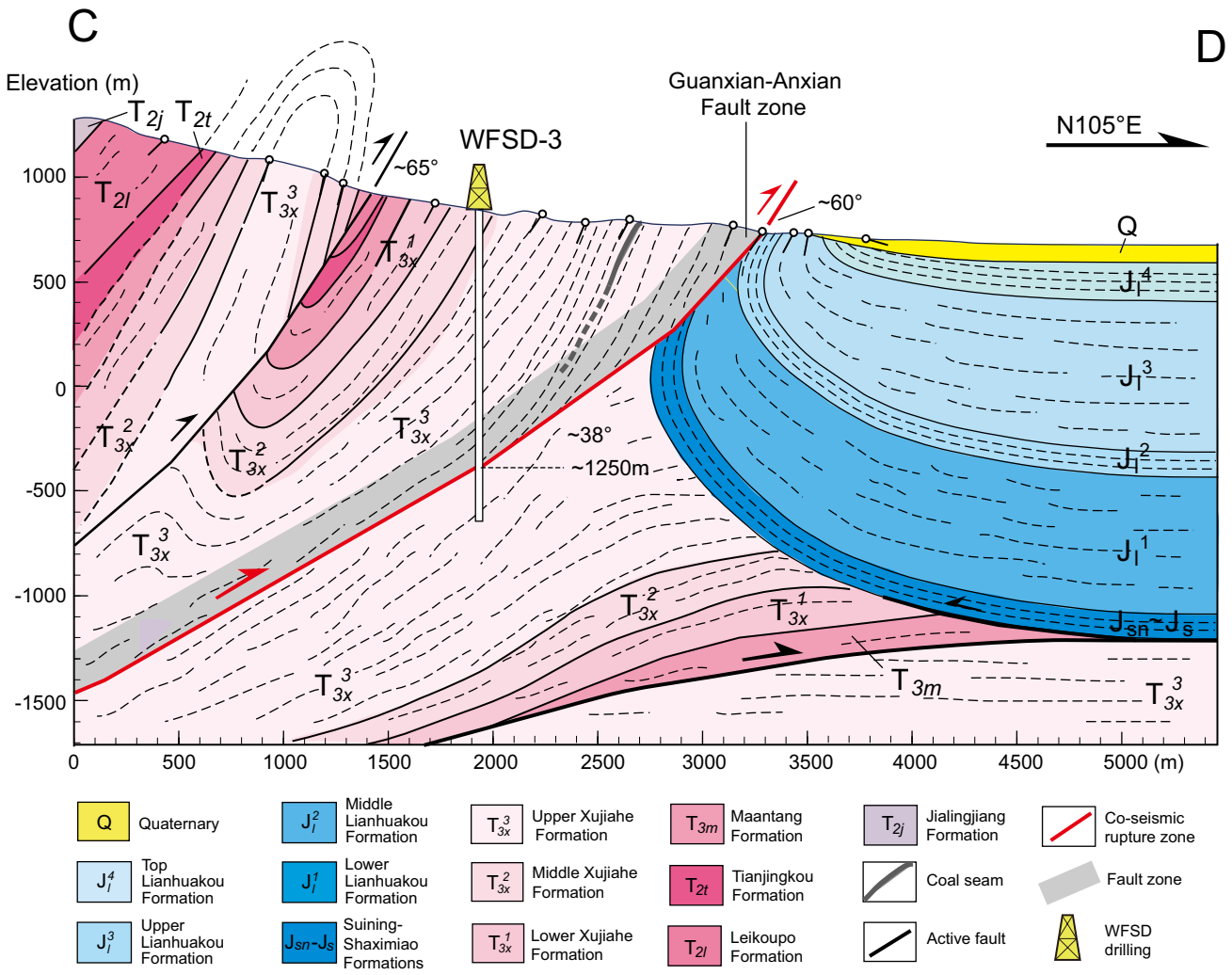

Fig. 14 Geological section across WFSD-3 drilling site and coseismic surface rupture zone of the Wenchuan earthquake. The width of the Guanxian–Anxian fault zone (*gray stripe*) is about 210 m. The surface rupture zone strikes ~N30°E and dips 60°NW at the *bottom* of the fault zone at the outcrop. The dip angle of the Guanxian–Anxian fault zone is about 38° at a depth of ~1250 m

the PSZ of the Wenchuan earthquake was not located at the bottom of the Yingxiu–Beichuan fault zone. In contrast, results from the WFSD-3 core analyses and outcrop observation show that the Guanxian–Anxian fault zone is ~210 m wide (~50 m fault rocks and ~160 m damage zone) with fault gouge thicknesses ranging from 1 mm to ~2.3 m. Along the Guanxian–Anxian fault zone, the rupture during the Wenchuan earthquake is a low-angle thrust fault with a dip angle of 60°–38° from the surface to 1250 m depth (Fig. 14). These two fault segments have different thicknesses and structures, which may suggest different faulting mechanisms.

Conclusions

Based on the detailed analyses of the 1502-m-long WFSD-3 cores and the logging data, as well as the field geological investigation, the following conclusions have been obtained:

1. Dark-gray sandstone, siltstone, argillaceous siltstone, carbonaceous–argillaceous siltstone, coal seam, liquefied breccia, fault breccia, and fault gouge are present in the WFSD-3 cores. At least 22 fault zones with various widths are recognized according to the fault rock distributions of the WFSD-3 cores. The thicknesses of the fault gouges range from 1 mm to 2.3 m.
2. The Guanxian–Anxian fault zone contains a zone of fault rocks and a damage zone characterized by fractures adjacent to the main fault. The zone of fault rocks has been identified in the WFSD-3 cores from 1192 to 1250 m depth with an actual width of ~50 m, while at the outcrop, it is ~40 m wide. The damage zone of the Guanxian–Anxian fault zone is ~160 m wide and is restricted in the hanging wall. Therefore, the actual total thickness of the Guanxian–Anxian fault zone in WFSD-3 cores is ~210 m.
3. Based on fault structure analyses in the WFSD-3 cores, as well as logging data, the PSZ of the Wenchuan earthquake was tentatively determined to be at the depth of 1249.95 m, located at the bottom of the Guanxian–Anxian fault zone, showing an asymmetrical fault structure. The slip plane of the Wenchuan earthquake along the Guanxian–Anxian fault zone is a low-angle thrust fault with a dip angle of 38° at the depth of 1249.95 m, while viewed from the surface outcrop, the dip angle of the slip plane is ~60°, which demonstrates the Guanxian–Anxian fault is a listric fault. These results show the Guanxian–Anxian fault is different from the Yingxiu–Beichuan fault, which is a high-angle thrust fault with a dip angle of ~65° studied from the WFSD-1. These two fault segments have different thicknesses and fault structures, which may suggest different faulting mechanisms for the Wenchuan earthquake.

Acknowledgments This research was supported by the National Science and Technology Planning Project of China, the Wenchuan earthquake Fault Scientific Drilling Project (WFSD), the National Natural Science Foundation of China (41330211, 41520104006) and the China Geological Survey project (12120114075801). We appreciate the help and support of Xuelong Wang, Shiyou Hu, Wei Zhang, Lasheng Fan, and Yixiong Niu of the Wenchuan earthquake Fault Scientific Drilling Project (WFSD) Center. Special thanks to the Faculty of the geological team 109, Bureau of Geology and Mineral Exploration of Anhui Province for their drilling work. We are grateful to Huihua Li, Yong Zhang, and Yuhang Wang from the geological team 405 for their excellent core logging work. We thank Shengli Well Logging Company of Sinopec Group and the Institute of Geophysical and Geochemical Exploration, Chinese Academy of Geological Sciences, for their borehole logging. We thank the three anonymous reviewers, Sheng-Rong Song, and Jim Mori for giving many useful comments and suggestions which greatly improved this manuscript.

References

Brodsky E, Ma KF, Mori J et al (2009) Rapid response fault drilling: past, present and future. Report of the ICDP/SCEC international workshop of rapid response fault drilling, Tokyo, Japan, 17–19 Nov

Burchfiel BC, Chen ZL, Liu Y et al (1995) Tectonics of the Longmen Shan and adjacent regions, Central China. Int Geol Rev 37(8):661–735

Chester FM, Mori J, Toczko S, Eguchi N, the Expedition 343/343T Scientists (2013) Japan Trench Fast Drilling Project (JFAST). In: IODP proceedings 343/343T

Chester FM, Logan JM (1986) Implications for mechanical properties of brittle faults from observations of the Punchbowl fault zone, California. Pure Appl Geophys 124:79–106

Densmore AL, Ellis MA, Li Y et al (2007) Active tectonics of the Beichuan and Pengguan faults at the eastern margin of the Tibetan Plateau. Tectonics. doi:10.1029/2006TC001987

Faulkner DR, Rutter EH (2003) The effect of temperature, the nature of the pore fluid, and subyield differential stress on the permeability of phyllosilicate-rich fault gouge. J Geophys Res Solid Earth 108(B5):567–572

Faulkner DR, Jackson CAL, Lunn RJ et al (2010) A review of recent developments concerning the structure, mechanics and fluid flow properties of fault zones. J Struct Geol 32:1557–1575

Fu BH, Wang P, Kong P et al (2008) Preliminary study of coseismic fault gouge occurred in the slip zone of Wenchuan Ms 8.0 earthquake and its tectonic implications. Acta Petrol Sin 24(10):2237–2243 **(in Chinese with English abstract)**

Fu BH, Shi PP, Wang P et al (2009) Geometry and kinematics of the Wenchuan earthquake surface ruptures around the Qushan Town of Beichuan County, Sichuan: implications for mitigation of seismic and geologic disasters. Chin J Geophys 52(2):485–495 **(in Chinese with English abstract)**

Fu BH, Shi PL, Guo HD et al (2011) Surface deformation related to the 2008 Wenchuan earthquake, and mountain building of the Longmen Shan, eastern Tibetan Plateau. J Asian Earth Sci 40(4):805–824

Fulton PM, Brodsky EE, Kano Y et al (2013) Low coseismic friction on the Tohoku-Oki fault determined from temperature measurements. Science 342:1214–1217. doi:10.1126/science.1243641

Gudmundsson A (2011) Rock fractures in geological processes. Cambridge University Press, Cambridge

Hirono T, Fujimoto K, Yokoyama T et al (2008) Clay mineral reactions caused by frictional heating during an earthquake: an example from the Taiwan Chelungpu fault. Geophys Res Lett. doi:10.1029/2008GL034476

Kano Y, Mori J, Fujio R et al (2006) Heat signature on the Chelungpu fault associated with the 1999 Chi–Chi, Taiwan earthquake. Geophys Res Lett. doi:10.1029/2006GL026733

Kuo LW, Song SR, Yeh EC et al (2009) Clay mineral anomalies in the fault zone of Chelungpu Fault, Taiwan, and its implication. Geophys Res Lett. doi:10.1029/2009GL039269

Kuo LW, Song SR, Huang L et al (2011) Temperature estimates of coseismic heating in clay-rich fault gouges, the Chelungpu fault zones, Taiwan. Tectonophysics 502(3–4):315–327

Kuo LW, Hsiao HC, Song SR et al (2014) Coseismic thickness of principal slip zone from the Taiwan Chelungpu fault Drilling Project-A (TCDP-A) and correlated fracture energy. Tectonophysics 619–620:29–35

Li Y, Zhou RJ, Densmore AL et al (2006) Geomorphic evidence for the late Cenozoic strike-slipping and thrusting in Longmen Mountain at the eastern margin of the Tibetan Plateau. Q Sci Rev 26(1):40–51 **(in Chinese with English abstract)**

Li HB, Fu XF, Van der Woerd J et al (2008) Co-seismic surface rupture and dextral-slip oblique thrusting of the Ms 8.0 Wenchuan earthquake. Acta Geol Sin 82(12):1623–1643 **(in Chinese with English abstract)**

Li HB, Si JL, Fu XF et al (2009) Co-seismic rupture and maximum displacement of the 2008 Wenchuan earthquake and its tectonic implications. Q Sci 29(3):387–402 **(in Chinese with English abstract)**

Li HB, Wang H, Xu ZQ et al (2013) Characteristics of the fault-related rocks, fault zones and the principal slip zone in the Wenchuan Earthquake Fault Scientific Drilling Project Hole-1 (WFSD-1). Tectonophysics 584:23–42

Li HB, Xu ZQ, Niu YX et al (2014) Structural and physical property characterization in the Wenchuan earthquake Fault Scientific Drilling project-hole 1 (WFSD-1). Tectonophysics 619–920:86–100

Lin AM, Maruyama T, Kobayashi K (2007) Tectonic implications of damage zone-related fault-fracture networks revealed in drill core through the Nojima fault, Japan. Tectonophysics 443:16–173

Liu J, Zhang ZH, Wen L et al (2008) The Ms 8.0 Wenchuan earthquake co-seismic rupture and its tectonic implications: an out of sequence thrusting event with slip partitioned on multiple faults. Acta Geol Sin 82(12):1707–1722 **(in Chinese with English abstract)**

Liu DL, Li HB, Lee TQ et al (2014) Primary rock magnetism for the Wenchuan earthquake fault zone at Jiulong outcrop, Sichuan Province, China. Tectonophysics 619–9620:58–69

Lu RQ, He DF, Suppe J et al (2012) Along-strike variation of the frontal zone structural geometry of the Central Longmen Shan thrust belt revealed by seismic reflection profiles. Tectonophysics 580:178–191

Ma KF, Tanaka H, Song SR et al (2006) Slip zone and energetics of a large earthquake from the Taiwan Chelungpu-fault Drilling Project. Nature 444(7118):473–476

Oshiman N, Shimamoto T, Takemura K et al (2001) Thematic issue: Nojima fault zone probe. Island Arc 10:195–505

Pei JL, Li HB, Sun ZM et al (2010) Fault slip in the Wenchuan earthquake fault belt—information from fault rocks with higher magnetic susceptibility. Q Sci 30(4):750–758 **(in Chinese with English abstract)**

Qiao XF, Guo XP, Li HB et al (2012) Soft-sediment deformation in the Late Triassic and the Indosinian tectonic movement in Longmenshan. Acta Geol Sin 86(1):132–156 **(in Chinese with English abstract)**

Si JL, Li HB, Kuo LW et al (2014) Clay mineral anomalies in the Yingxiu-Beichuan fault zone from the WFSD-1 drilling core and its implication for the faulting mechanism during the 2008 Wenchuan earthquake (Mw 7.9). Tectonophysics 619–620:171–178

Sibson RH (1977) Fault rocks and fault mechanisms. J Geol Soc 133(3):191–213

Sibson RH (2003) Thickness of the seismic slip zone. Bull Seismol Soc Am 93(3):1169–1178

Sichuan Bureau of Geology and Mineral Resources (1996) Geologic map of Mianzhu (scale 1:50000) **(in Chinese)**

Song SR, Kuo LW, Yeh EC et al (2007) Characteristics of the lithology, fault-related rocks and fault zone structures in the TCDP Hole-A. TAO 18:243–269

Spray JG (1995) Pseudotachylyte controversy: Fact or friction? Geology 23(12):1119–1122

Wang H, Li HB, Si JL et al (2014) Internal structure of the Wenchuan earthquake fault zone, revealed by surface outcrop and WFSD-1 drilling core investigation. Tectonophysics 619–620:101–114

Wang H, Li HB, Janssen C et al (2015) Multiple generations of pseudotachylyte in the Wenchuan fault zone and their implications for coseismic weakening. J Struct Geol 74:159–171

Xu ZQ, Ji SC, Li HB et al (2008) Uplift of the Longmen Shan range and the Wenchuan earthquake. Episodes 31(3):291–301

Xu XW, Wen XZ, Yu GH et al (2009) Coseismic reverse- and oblique-slip surface faulting generated by the 2008 Mw 7.9 Wenchuan earthquake, China. Geology 37(6):515–518

Yu GH, Xu XW, Klinger Y et al (2010) Fault-scarp features and cascading-rupture model for the Mw 7.9 Wenchuan earthquake, eastern Tibetan plateau, China. Bull Seismol Soc Am 100(5B):2590–2614

Zoback MD, Hickman S, Ellsworth W (2007) The role of fault zone drilling. Geophysics 4:649–674